Electric Field Gradient Calculations of Various Borides *

K. Schwarz, H. Ripplinger, and P. Blaha

Institut für Technische Elektrochemie, Technische Universität Wien, Getreidemarkt 9/158, A-1060 Vienna, Austria

Z. Naturforsch. **51a**, 527–533 (1996); received October 10, 1995

A first-principles method for the computation of electric field gradients (EFG) is illustrated for various borides. It is based on energy band calculations using the full-potential linearized augmented plane wave (LAPW) method within density functional theory. From the self-consistent charge density distribution the EFG is obtained without further approximations by numerically solving Poisson's equation. The dependence of the EFG on structure, chemical composition or substitution is demonstrated for the diborides MB_2 (with M = Ti, V, Cr, Zr, Nb, Mo, and Ta), the hexaborides (CaB_6, SrB_6 and BaB_6) and boron carbide which is closely related to α-boron.

Key words: Band-structure calculations, Electric field gradient, Diborides, Hexaborides, Boron carbide.

Introduction

Several experimental techniques like nuclear quadrupole resonance (NQR), nuclear magnetic resonance (NMR), Mössbauer or perturbed angular correlation (PAC) spectroscopy allow the determination of hyperfine interaction parameters. All nuclei with a nuclear-spin quantum number $I > 1/2$ have a nonvanishing nuclear quadrupole moment Q and thus the nuclear quadrupole coupling constant (NQCC) eQV_{zz}/h, where e is the electric charge, h is Planck's constant and V_{zz} represents the electric field gradient (EFG), can be determined by one of the methods mentioned above. The EFG is a ground state property of a system and depends sensitively on the electronic charge distribution in the vicinity of the probe nucleus. Therefore such measurements can provide valuable information on the chemical bonding in solids provided an interpretation of the measured quantities is possible. In order to obtain better insight into the connection between EFG, charge distribution and chemical bonding, a calculation of these quantities and a thorough analysis is very helpful.

Over the last decade we have developed a method to calculate EFGs in solids based on accurate band structure calculations [1]. We have applied this procedure to various systems including the hcp metals [2], ionic systems like Li_3N [1] or TiO_2 [3], the high T_c superconductor [4] or molecular crystals of Cl_2, Br_2, and I_2 [5]. These calculations did no just reproduce the experimental EFG very well but also provided new insight into the physical origin of the EFG.

In the present paper we focus on first principles calculations of the EFG at boron sites of several boron compounds. We select borides with the AlB_2 or CaB_6 structure, α-boron and boron carbide and compare our results with experimental EFGs and related data.

Method

We use the full potential linearized-augmented-plane-wave (LAPW) method as embodied in the WIEN95 code [6] in a scalar relativistic version without spin-orbit coupling, which is one of the most accurate schemes available. All convergence parameters must be well controlled such as the basis set in terms of plane waves, l_{max} of various spherical harmonics expansions or the k-points for the Brillouin zone sampling (for details see reference 6). Exchange and correlation effects are treated within density functional theory (DFT) using both, the common local spin density approximation (LSDA) and the recent improvement in form of the generalized gradient approximation (GGA) [7]. The latter was found superior to standard LSDA for determining equilibrium volumes (positions) by total energy minimization which also leads to the correct ground state in some transition metal

* Presented at the XIIIth International Symposium on Nuclear Quadrupole Interactions, Providence, Rhode Island, USA, July 23–28, 1995.

Reprint requests to Prof. Dr. Karlheinz Schwarz.
kschwarz@email.tuwien.ac.at

0932-0784 / 96 / 0500-0527 $ 06.00 © – Verlag der Zeitschrift für Naturforschung, D-72072 Tübingen

compounds [8] and gives more accurate electron density distributions.

Once the electron density $\varrho(\boldsymbol{r})$ is calculated self-consistently and accurately, the EFG can be obtained from $\varrho(\boldsymbol{r})$ without further approximations. For instance, the principal component V_{zz} of the EFG tensor is given by

$$V_{zz} = \int \varrho(\boldsymbol{r}) \frac{2P_2(\cos\Theta)}{r^3} \mathrm{d}\boldsymbol{r},$$

where P_2 is the second-order Legendre polynomial. It was shown previously [2] that in many cases the main contribution to this integral comes from a region close to the nucleus of the respective atom. Thus it is often meaningful to decompose the EFG contributions into terms from the atomic sphere surrounding the respective nucleus and the rest of the unit cell. The former part can be further analyzed in terms of p-p and d-d contributions corresponding to the product of two l-like radial wave functions. For example, the p-p EFG contribution is proportional to

$$V_{zz}^{p} \propto \Delta n_{p_z} \left\langle \frac{1}{r^3} \right\rangle_p,$$

where $\langle 1/r^3 \rangle$ is the respective expectation value of the p-wavefunctions and the Δn_p is the anisotropy count defined as

$$\Delta n_{p_z} = p_z - \frac{p_x + p_y}{2},$$

where p_x, p_y, and p_z are the respective partial charges inside the corresponding atomic sphere.

Such a decomposition characterizes the physical origin of the EFG and allows to determine whether the EFG stems from valence p- or d-like states (for boron of course only p states are important), to which extent the $\langle 1/r^3 \rangle$ expectation value (i.e. the radial wavefunction) remains constant and how the EFG is connected to the charge anisotropy (Δn_p) related to chemical bonding.

Results

Diborides

For the calculation of EFGs in the diborides of AlB_2-type (space group P6/mmm) we take the experimental volume and c/a ratio from Silver and Kushida [9]. At this volume we optimized the c/a ratio by total energy minimization and found that it lies within 2% of the experimental value. The calculated EFGs at the B and Me sites of various diborides are compared to available experimental data (Table 1). The B-EFG is small but varies by more than an order of magnitude between compounds in excellent agreement with the experimentally measured quantities. The results for the Me-EFG are also included in Tab. 1, although the only experimental value available is that for ^{51}V which agrees well with theory. For all other Me-EFGs we make a theoretical prediction. It should be mentioned, that all values quoted in Table 1 are obtained within LSDA and the differences to GGA calculations are less than 3% for all B-EFG except for TaB_2 where the EFG is extremely small.

Table 1. Experimental and theoretical EFG (in 10^{21} V/m^2) for the boron (V_{zz}^{B}) and metal (V_{zz}^{Me}) sites in various diborides. The lattice parameters for the calculation and the experimental NQCC are taken from Silver and Kushida [9] and the latter are converted into EFGs using $Q = +0.04058$ b for ^{11}B and $Q = -0.052$ b for ^{51}V [23].

Compound	exp. V_{zz}^{B}	theor. V_{zz}^{B}	exp. V_{zz}^{Me}	theor. V_{zz}^{Me}
TiB_2	0.37 ± 0.02	0.38		2.20
VB_2	0.43 ± 0.01	0.39	1.87 ± 0.14	1.71
CrB_2	0.63 ± 0.01	0.60		0.84
ZrB_2	0.12 ± 0.01	0.10		4.68
NbB_2	< 0.07	0.10		5.03
MoB_2	0.23 ± 0.02	0.22		2.28
TaB_2	< 0.05	0.02		9.56

The hexaborides CaB_6, SrB_6 and BaB_6

The next examples we choose are the hexaborides (space group Pm3m) with the CaB_6 structure displayed at the top of Figure 1. This figure shows for BaB_6 (at the experimental volume) how various quantities depend on the internal parameter x. The top panel displays the total energy as function of x with a minimum at $x = 0.2057$. The hexaborides are often considered to consist of boron octahedra as essential building blocks which are linked around a central metal atom, but at the equilibrium volume the inter-octahedral B-B distance (BB1) is smaller than the intra-octahedral one (BB2) (see bottom panel of Figure 1). Therefore these compounds contain as crucial elements also B-B dimers (dumb-bells) which have an even shorter boron-boron distance than inside the B octahedron. In order to investigate the pressure sensitivity on the EFG we have varied the volume and

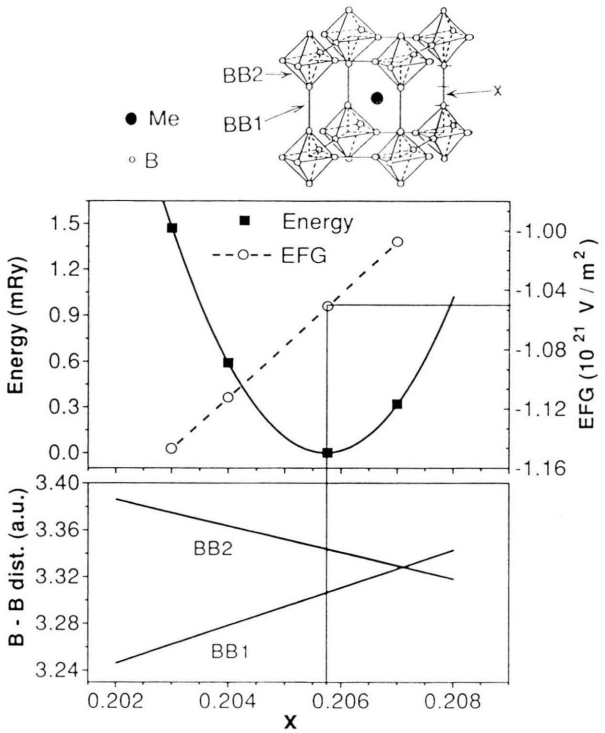

Fig. 1. CaB_6 structure showing the inter- (BB1), the intra-octahedral distance (BB2), and the internal parameter x. For BaB_6 the total energy (with respect to its minimum), the electric field gradient (EFG) for boron are shown (top panel) as a function of x, together with BB1 and BB2 (bottom panel).

relaxed the x-parameter. The EFG varies linearly with x by several percent (top of Figure 1). Under pressure the BB1 distance decreases more than BB2, although BB1 is smaller (at the equilibrium volume) than BB2 suggesting a stronger (stiffer) bonding in the dumbbells than within the octahedra. This behaviour may be explained by considering that each boron forms four bonds within one octahedron but only one to the neighboring octahedron so that under compression the four bonds dominate.

In Tab. 2 a comparison between theoretical and experimental EFGs for CaB_6, SrB_6 and BaB_6 is made. The theoretical results show a clear trend (Fig. 2) of a decreasing EFG when going from Ca to Ba, but this trend is not confirmed by experiment (Table 2) [10]. One possible reason for this discrepancy could be the nonstoichiometry that may have affected the EFG measurements which show a significant spread in their data, especially for CaB_6 [11, 12]. Therefore we encourage new measurements on well characterized samples.

Despite these descrepancies between theory and experiment we rely on our theoretical results and analyze how the EFG is affected by various parameters. The influence on the B-EFG in this class of compounds is illustrated for three different parameters namely i) the volume of the unit cell, ii) the relaxation of the internal structural parameter x that determines the distances between the boron atoms, and iii) the substitution of the metal atom (Me) at the center of the cubic unit cell (i.e. the chemical effect of the central atom). For this purpose we performed several calcula-

Table 2. Experimental [10] and theoretical EFGs (in 10^{21} V/m^2) in some hexaborides.

	exp. V_{zz}^B	theor. V_{zz}^B
CaB_6	1.28 ±0.02	1.36
SrB_6	0.57 ±0.08	1.22
BaB_6	0.814±0.04	1.05

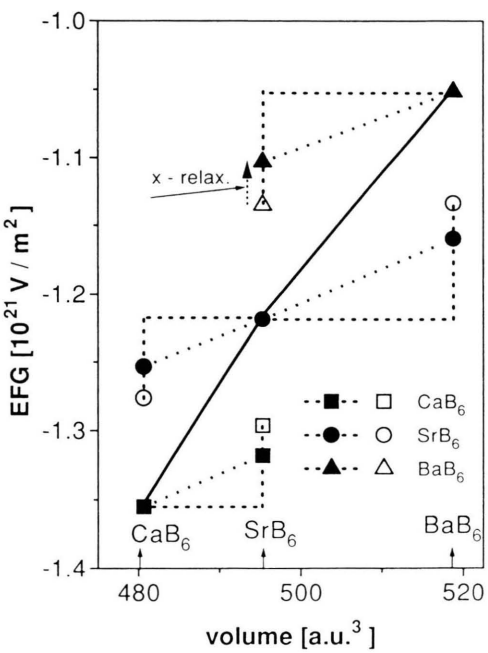

Fig. 2. The electric field gradient (EFG) at the boron site for the hexaborides CaB_6, SrB_6, and BaB_6 as a function of volume. The solid line conects the EFG values coresponding to the respective equilibrium volumes. The EFG for relaxed x parameters are denoted with full symbols, while open symbols characterize cases, where Me is substituted but all structural parameters of the host are kept fixed.

tions varying the volume, the internal parameter x, and the Me-substitution. For the experimental structure (experimental equilibrium volume and relaxed x-parameters) the EFG varies by about 30% between CaB_6 and BaB_6 (solid line in Figure 2). This variation can be associated with the three factors mentioned above. For example, if one compresses BaB_6 to the volume of SrB_6 and keeps x fixed, the EFG is changed by about 1% but when x is relaxed (full triangle at $V = 488$ a.u. [3]) the EFG changes from -1.05 to -1.10 [10^{21} V/m^2]. However, starting from the SrB_6 phase (without any change in structural parameters) and substituting Sr by Ba changes the EFG to -1.14 (open triangle), while SrB_6 itself (full circle) has an EFG of -1.22 [10^{21} V/m^2]. Therefore the substitution of the Me-atom is responsible for about half the effect on the EFG, while the relaxation of the x-parameter accounts for the rest, where about one quarter is the relaxation at constant volume (due to substitution) and another quarter is a consequence of the change in volume (again caused by the substitution). A change in volume without substitution and relaxation has very little effect. The other cases included in Fig. 2 show similar trends, where the full symbols depict relaxed geometric parameters at various volumes while the open symbols indicate substitutions without any relaxation.

A spatial decomposition of the EFG contributions can be used to further analyze the results as mentioned in the previous section. We find that the EFG in these hexaborides originates only to about 60% from within the boron sphere (with a radius of 1.5 a.u.) while the remaining part to the EFG comes from the interstitial region. This relatively small fraction from the respective boron sphere is consistent with previous results, e.g. for hcp Be [2] or for oxygen EFGs in the high T_c superconductors [4], where the rule has been established that the EFG is dominated by the region near the nucleus till the first radial node. Therefore for a first-row element (with a nodeless and fairly delocalized B-2p wavefunction) contributions from outside the sphere can not be neglected. For all heavier elements, however, the largest part of the EFG originates from the small region of the valence wavefunctions up to the first radial node [2, 4].

For borides the EFG comes mostly from the asymmetry of the 2p electrons and the excess p_z charge (z along the B_2 dumb-bell) leads to an asymmetry count Δn_p of about 0.1 e, indicating stronger covalent bonds within the boron dumb-bell. In all three hexaborides the EFG is strictly proportional to Δn_p leading to a constant $\langle 1/r^3 \rangle$ expectation value of about 13 a.u. (including all proportionality factors). The largest charge anisotropy and thus the highest EFG is found in CaB_6.

Boron carbides (B_4C-type)

Boron carbide is closely related to α-boron which consists of B_{12} icosahedra in a rhombohedral structure (space group $R\bar{3}m$) between which a chain of three atoms is inserted leading to $B_{12}C_3$ often denoted as B_4C [13]. The stoichiometry is not always fixed and this chain most probably does not consist of three C atoms (CCC), but other arrangements such as (CBC) are also favoured in literature [14], where the extra C statistically replaces one of the boron atoms in the icosahedron [14, 16] so that X-ray diffraction would not be able to detect a break of the rhombohedral symmetry [15]. For $B_{13}C_2$ Emin and others concluded from their analysis of free energy [16], Raman spectra [17], electron-spin resonance [18], thermal conductivity [19], conductivity by bipolaron-hopping, Seebeck coefficient, and electronic conductivity [19], that the correct structure is $B_{11}C$ (BBC), while Bylander and others [14] assume a B_{12} (CBC) structure.

For our calculations we take the crystallographic data from Kirfel et al. [20]. In order to model some of these disordered boron carbides we restrict ourselves to configurations with inversion symmetry so that we retain real matrix elements of the corresponding hamiltonian, a significant computational advantage over the non-centro-symmetric case with complex arithmetic. Since this system is rather complicated, at present we can report only first results. We choose $B_{12}(B_xC_y)$ and investigate the EFGs in B_{12}, B_{12}(BCB), B_{12}(CBC) and B_{12}(CCC) for which we optimized the 5 (4 in B_{12}) free positional parameters by minimizing the forces acting on the atoms (for fixed cell dimensions taken from $B_{13}C_2$).

Table 3 gives the theoretical B-EFG (and the C-EFG in square brackets) for various configurations together with the experimental data [21] for B_4C. The largest experimental value of 5.68 [10^{21} V/m^2] was attributed to the center of the chain, while the two smaller ones were interpreted to come from the B icosahedron. We find such a large B-EFG for the central B position (site 1 b) of the chain, while the end position of the chain (site 2c) would have a much smaller value. The EFGs at the two types of icosahe-

Table 3. Theoretical EFGs [10^{21} V/m^2] for α-B_{12} and some icosahedral boron carbides. The labels (BCB), etc. indicate the occupation of the chain positions between the icosahedra. Values in parentheses are for carbon, the experimental values [21] are for B in B_4C,

Position	α-B_{12}	B_{12}(BCB)	B_{12}(CBC)	B_{12}(CCC)	exp. B_4C
B[C]-1b	–	[−10.31]	−5.83	[−8.72]	5.68 ± 0.02
B[C[-2c	–	−1.21	[−1.30]	[−0.25]	
B-6h1	0.88	0.24	−0.51	0.54	0.71 > EFG > 0.2*
B-6h2	−1.54	−1.14	−0.69	−1.33	1.32 ± 0.1*

* Assuming asymmetry parameter $\eta = 0$.

dral sites (6h1, 6h2) are in good agreement with experiment for B_{12}(CCC), but every substitution of these three C atoms in the chain by B would lead to an EFG at the 6h2 position that is smaller than the experimental value. Thus we can partly confirm the experimental assignment, in particular the largest EFG from the boron in the center of the chain. We note that the EFGs at the equatorial and axial positions within the icosahedron (6h1 and 6h2) are much smaller but differ significantly upon insertion or substitution of the chain. They are also very sensitive to small structural changes so that a structure optimization was essential. Therefore in terms of the electronic distribution the icosahedron is not a rigid entity with respect to the EFG but is affected by the presence of the chain atoms. These EFG values are of comparable magnitude to that of boron at the end of the chain.

The density-of-states (DOS) curves (Fig. 3) for the icosahedral boron atoms in α-B_{12}, B_{12}(CBC), and B_{12}(CCC) show an overall similarity. The main differences come from the DOS of the additional chain atoms which are also displayed for the latter two cases. For example in B_{12}(CBC) an additional feature appears in the region −0.37 to −0.50 (Ry), which originates mainly from states of the chain atoms, but an admixture of these states in the region 0.1 to 0.35 (Ry) is also apparent, where otherwise the B_{12} DOS dominates. This type of interaction is the reason why the EFG at the icosahedron is sensitive to the chain atoms as discussed above. Both, B_{12} and B_{12}(CCC) within our model structure, are insulators, while B_{12}(CBC) is found to be metallic due to an odd number of valence electrons.

The asymmetry count Δn_p of the chain boron atom in B_{12}(CBC) can be obtained as a function of energy (Fig. 4) by filling the corresponding partial DOS. The large Δn_p value (solid curve) up to the Fermi energy

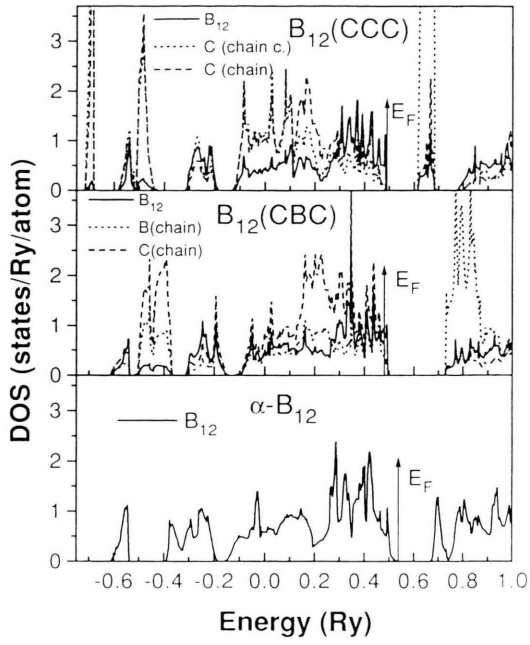

Fig. 3. Partial density of states (DOS) curves of α-B_{12} and two model systems for boron carbide, namely B_{12}(CBC) and B_{12}(CCC). The partial DOS of the icosahedron (averaged) and the chain atoms (center and outer position) are shown.

E_F shows that p_z dominates over p_x and p_y, where the z direction points towards the carbon neighbours in the CBC chain. Above the gap (around 0.72 Ry) these partial DOS come almost exclusively from the p_x and p_y orbitals and thus would result in a change of sign in Δn_p. An analysis shows that about 80% of the EFG originates from the contributions of the B sphere of 1.3 a.u. and the respective $\langle 1/r^3 \rangle_p$ proportionality factor is 21.5 a.u., much larger than in the hexaborides.

In order to estimate the sensitivity of the large EFG (from the central B-chain atom) to stoichiometry effects, a rigid band model can be used for B_{12}(CBC). If we add or substract one electron from the valence (but keep the partial DOS) the resulting V_{zz} component of the EFG changes only by ±3%, so that we can conclude that this EFG is relatively insensitive to the position of the Fermi energy.

Conclusion

We have calculated the EFGs for seven AlB_2-type diborides and the results agree well with experimental

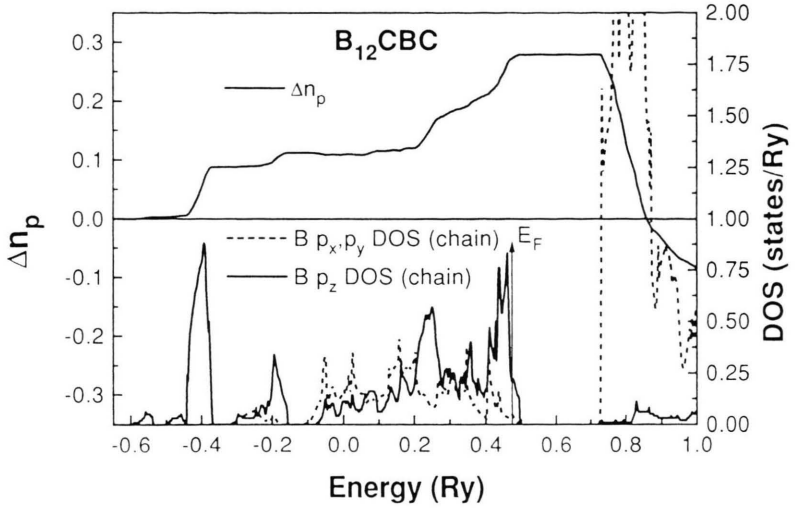

Fig. 4. Asymmetry count Δn_p and the respective partial density of states (DOS) curves of boron at the center of the chain in $B_{12}CBC$.

data. The small differences in EFGs calculated within LSDA or GGA show that here the treatment of exchange-correlation effects is not as crucial as in other cases as for example in Fe compounds [22].

In a series of three alkaline earth CaB_6 type hexaborides we have shown how volume and relaxation of the internal parameter affects the EFG. The central atom has a larger effect on the EFG than volume and relaxation. We have interpreted the EFG in terms of the asymmetry of the charge distribution related to the occupation numbers of p_z and p_x, p_y states of boron. Good agreement with one experimental result for CaB_6 is obtained, but considerable deviations occur for SrB_6 and some for BaB_6. This calls for new NMR measurements on SrB_6 and BaB_6 using well characterized samples with good stoichiometry.

We have calculated EFGs in α-B_{12} and B_4C. Model calculations for B_{12}(CBC) and B_{12}(CCC) show the sensitivity of the EFG on structure and charge redistribution. In boron carbide we concentrate on the chain of three atoms inserted in between the B_{12} icosahedra and can clearly distinguish between the positions, since the EFGs of the central and end atoms of the chain differ significantly. For a better understanding of the boron carbide system, additional calculations with an appropriate analysis and new experiments would be needed.

Acknowledgement

This work was supported by the *"Hochschuljubiläumsstiftung der Stadt Wien"*.

[1] P. Blaha, K. Schwarz, and P. Herzig, Phys. Rev. Lett. **54,** 1192 (1985).
[2] P. Blaha, K. Schwarz, and P. H. Dederichs. Phys. Rev. **B37,** 2792 (1988).
[3] P. Blaha, D. J. Singh, P. I. Sorantin, and K. Schwarz, Phys. Rev. **B46,** 1321 (1992).
[4] K. Schwarz, C. Ambrosch-Draxl, and P. Blaha. Phys. Rev. **B42,** 2051 (1990).
[5] P. Blaha and K. Schwarz, J. Mol. Struct. (Theochem), **261,** 355 (1992).
[6] P. Blaha, K. Schwarz, P. Dufek, and R. Augustyn, WIEN95, Technical University of Vienna, 1995. (An improved and updated Unix version of the original copyrighted WIEN-code, which was published by P. Blaha, K. Schwarz, P. I. Sorantin, and S. B. Trickey, Comput. Phys. Commun. **59,** 399 (1990).
[7] J. P. Perdew, In: *Electronic structure of Solids* '91, eds. P. Ziesche and H. Eschrig (Akademie Verlag, Berlin 1991).
[8] P. Dufek, P. Blaha, V. Sliwko, and K. Schwarz, Phys. Rev. **B49,** 10170 (1994).
[9] A. H. Silver and T. Kushida, J. Chem. Phys. **38,** 865 (1963).
[10] R. E. Sears, J. Chem. Phys. **76,** 5651 (1982).
[11] M. Aono and S. Kawai, J. Phys. Chem. Solids **40,** 797 (1979).
[12] T. Kushida, N. Laurance, and A. H. Silver, Bull. Am. Phys. Soc. **7,** 226 (1962).
[13] D. M. Bylander, L. Kleinman, and S. Lee, Phys. Rev. **B42,** 1394 (1990).
[14] S. Lee, S. W. Kim, D. M. Bylander, and L. Kleinman, Phys. Rev. **B44,** 3550 (1991).

[15] D. M. Bylander and L. Kleinman, Phys. Rev. **B 43,** 1487 (1991).
[16] D. Emin, Phys. Rev. **B 38,** 6041 (1988).
[17] D. R. Tallant, T. S. Aselage, A. N. Campbell, and D. Emin, Phys. Rev. **B 40,** 5649 (1989).
[18] E. L. Venturini, D. Emin, and T. L. Aselage, and C. Wood, Materials Research Society, Pittsburgh, 1987, p. 83.
[19] C. Wood and D. Emin, Phys. Rev. **B 29,** 4582 (1985).
[20] A. Kirfel, A. Gupta, and G. Will, Acta Cryst. B **35,** 1052 (1979).
[21] A. H. Silver and P. J. Bray, J. Chem. Phys. **31,** 247 (1959).
[22] P. Dufek, P. Blaha, and K. Schwarz. Phys. Rev. Lett. **75,** 3545 (1995).
[23] P. Pyykkö, Z. Naturforsch. **47 a,** 189 (1992).